Effects of dissolved oxygen, pH, and anions on the 2,3-dichlorophenol degradation by photocatalytic reaction with anodic TiO_2 nanotube films

Hai-chao Liang[a], Xiang-zhong Li[a,*], Yin-hua Yang[b], Gang-hong Sze[b],

[a] *Department of Civil and Structural Engineering, The Hong Kong Polytechnic University, Hong Kong, China*

[b] *Departmernt of Chemistry, The Hong Kong University, Hong Kong, China*

**Corresponding author. Tel.: +852 2766 6016; Fax: +852 2334 6389.*

E-mail address: cexzli@polyu.edu.hk

Abstract

In this study, the highly-ordered TiO_2 nanotube (TNT) arrays on titanium sheets were prepared by an anodic oxidation method. Under UV illumination, the TNT films demonstrated the higher photocatalytic activity in terms of 2,3-dichlorophenol (2,3-DCP) degradation in aqueous solution than the conventional TiO_2 thin films prepared by a sol-gel method. The effects of dissolved oxygen (DO) and pH on the photocatalytic degradation of 2,3-DCP were investigated. The results showed that the role of DO in the 2,3-DCP degradation with the TNT film was significant. It was found that 2,3-DCP in alkaline solution was degraded and dechlorinated faster than that in acidic solution whereas dissolved organic carbon removal presented an opposite order in dependence of pH. In the meantime, some main intermediate products from 2,3-DCP degradation were identified by a ^{1}H-NMR technique to explore a possible degradation pathway. A major intermediate, 2-chlororesorcinol, was identified from the 2,3-DCP decomposition as a new species compared to the findings in previous reports. Photocatalytic deactivation was also evaluated in the presence of individual anions (NO_3^-, Cl^-, SO_4^{2-}, and $H_2PO_4^-$). The inhibition degree of photocatalytic degradation of 2,3-DCP caused by these anions can be ranked from high to low as $SO_4^{2-} > Cl^- > H_2PO_4^- > NO_3^-$. The observed inhibition effect can be attributed to the competitive adsorption and the formation of less reactive radicals during the photocatalytic reaction.

Keywords: Anion; Dissolved oxygen; Photodegradation; TiO_2 nanotube; 2,3-Dichlorophenol

1. Introduction

The halogenated aromatics in aquatic bodies are mainly from industrial wastewater and chlorination process of water purification and have been known to cause severe pollution problems (Bellar et al., 1974; Kinzell et al., 1979; Ku et al., 1996). Dichlorophenols (DCP), such as 2,3-DCP, 2,4-DCP, 2,5-DCP, and 2,6-DCP, have limited degradation by most conventional biological processes due to their toxicity (Zheng et al., 2004; Ye and Shen, 2004). The photocatalysis with immobilized TiO_2 thin films is an alternative to using TiO_2 powder with ease of separating TiO_2 catalyst from aqueous suspension (Arabatzis et al., 2002; Gracia et al., 2004). However, this process has limited surface area with the declined efficiency of photocatalytic reaction compared to using TiO_2 powder in aqueous suspension. Therefore, synthesis of the TiO_2 films with larger surface area and a better structure is a key step for its practical application.

Recently TiO_2 nanotube films have gained great attraction due to their large surface area, good mechanical adhesion strength, and high electronic conductivity. The immobilized TiO_2 nanotube films can be prepared by an anodic oxidation method through direct growth on titanium metal. As a result, this not only develops a new way to engineer TiO_2 nanostructures, but also explores wide applications in solar energy conversion (Hahn et al., 2007), water splitting (Mor et al., 2005), gas sensors (Mor et al., 2006), and environment purification (Quan et al., 2005; Zhuang et al., 2007). Quan et al. (2005) reported that the degradation of pentachlorophenol using an anodic TiO_2 nanotube film with large surface area was much faster than that using a traditional TiO_2 thin film formed by a sol-gel method. Xie (2006) reported that an anodic TiO_2/Ti nanotubular film as a photoanode exhibited a good reactivity for the photoelectrocatalytic degradation of bisphenol A in aqueous solution. However, these works were mainly focused on the aspect of material science, but the effects of key reaction conditions such as dissolved oxygen (DO), pH, and the anions commonly contained in wastewater on the photocatalytic reaction of using the TiO_2 nanotube films have not well been investigated.

It is well known that DO can act as an electron acceptor to eliminate the recombination of photogenerated electron-hole pairs and the nanotubular TiO_2 surface with better separation of electrons and holes allows more efficient channeling of the charge carriers into useful reduction and oxidation reactions. On the other hand, the presence of various inorganic anions such as SO_4^{2-}, Cl^-, $H_2PO_4^-$, and NO_3^- coexisting in various industrial effluents may cause some negative effects on the photocatalytic decomposition of organic compounds (Chen et al., 1997; Hu et al., 2003).

These anions are likely to retard the rates of organic compound oxidation by bidding for oxidizing radicals or by blocking the active sites of the TiO_2 catalyst. Therefore, this study aims at evaluating the influence of DO, pH, and selected inorganic anions on the photocatalytic degradation of 2,3-DCP in aqueous solution using the anodic TiO_2 nanotube films under UV light irradiation.

2. Experimental

2.1. Materials

Titanium foils (140 μm thickness, 99.6% purity) were purchased from Goodfellow Cambridge Ltd. as a raw material to prepare TiO_2 nanotube films. 2,3-DCP chemical with analytical grade was obtained from Aldrich Chemical Company and employed as a model pollutant. Deionized distilled water (DDW) was used throughout the experiments.

2.2. Anodic oxidation process

A large piece of raw Ti foil was cut into small rectangle pieces of 30 mm × 10 mm each, which were ultrasonically cleaned in acetone-ethanol solution and then rinsed by DDW as the prepared Ti foil samples. The anodic oxidation process was performed in a two-electrode cell, in which the prepared Ti foil was used as the anode and a platinum foil with the same size was employed as the cathode. Both the electrodes were submerged in aqueous 0.1 M NH_4F electrolyte solution with an initial pH 1.5 and were connected with a regulated DC power supply (Kikusui Electronic Corp. Japan, PAC 35-5). All anodization experiments were conducted at a constant electrical potential of 25 V and lasted for 1 h. The freshly anodized TiO_2/Ti foil was washed by DDW and further calcined at 500 ^{o}C for 1 h. The product TiO_2 nanotubular films were named "TNT" films.

2.3. Experimental

One piece of TNT films with an area of 3 cm^2 was placed in a single-compartment reactor filled with 25 mL of aqueous 2,3-DCP solution (20 mg L^{-1}) and an 8-W medium-pressure mercury lamp with a main emission at 365 nm (Institute of Electrical Light Source, Beijing, China) was applied as an external UV light source. A distance between the lamp and the top surface of the solution is 6 cm. Prior to photoreaction, the 2,3-DCP solution was magnetically stirred in the dark for 60 min in order to achieve adsorption/desorption equilibrium. The reaction systems were aerated

continuously with an air flow, unless otherwise mentioned. During the photoreaction, samples were collected from the solution at different intervals for analyses.

2.4. Characterization and chemical analysis

The surface morphology and element composition of the anodic TNT films were first examined by the field-emission scanning electron microscopy (FESEM) and X-ray diffraction measurement (XRD, with a Bruker D8 Discover X-ray diffractometor). To investigate the surface charges of photocatalysts in aqueous solution, zeta potential measurements were carried out using a Malvern Zetasizer 3000 (Malvern, UK). TiO_2 nanotubes were peeled off from TNT films to obtain TNT powder and then the TNT powder was used to prepare it suspension with a concentration of 0.1 g L^{-1} in aqueous solution and dispersed ultrasonically for 2 h. Degussa P25 was also used to prepare its suspension with the same concentration for comparison. The 2 M HCl and 2 M NaOH solutions were used to adjust pH to the desired values. As a result, the isoelectric point of the catalysts was obtained by the measurement of the zeta-potential. 2,3-DCP concentration was analyzed by HPLC (Finnigan SpectraSYSTEM P4000) consisting of a Pinnacle II C18 reverse-phase column (5 μm, 4.6 mm × 250 mm) and a UV detector (UV 6000LP). The mobile phase of acetonitrile/water (v:v = 3:2) was flowed at 1.0 mL min^{-1}. The concentration of dissolved organic carbon (DOC) was determined by a total organic carbon analyzer (Shimadzu TOC-5000A). Chloride ions released from the 2,3-DCP degradation were determined by spectrophotometry at 460 nm after the reaction with mercury thiocyanate.

In order to unambiguously identify the intermediate products of 2,3-DCP degradation, ^{1}H-NMR analysis, a special feature of this study versus previous contributions (D'Oliveira et al., 1993), was employed, in which 2,3-DCP solutions of 300 mg L^{-1} were used in photocatalytic experiments and 1 mL of each sample was taken in a NMR tube at different time intervals.

3. Results and discussion

3.1. Morphology and structure of TNT film

The morphology of TNT film was first examined by FESEM and its image is shown in Fig. 1a. It can be seen that the TNT film has a tubular porous structure, on which TiO_2 nanotubes were well-aligned as uniform arrays with high density. While the inner diameter of the nanotubes was

about 100 nm, the tube length was about 0.31 μm and the wall thickness was 28 nm on average. The XRD pattern of the TNT film calcined at 500 ^{o}C was analyzed and compared with that of Ti foil, as shown in Fig. 1b. The TNT film had characteristic peaks at 25.35^{o} (101), 27.5^{o} (110), 36.1^{o} (101), 48.1^{o} (200), 54.3^{o} (211), and 69.8^{o} (220), respectively. According to the XRD indexation, the crystal form of TNT is a mixture of rutile and anatase phases in good agreement with previous reports (Uchikoshi et al., 2004; Eder et al., 2006). From the FESEM and XRD results, it can be confirmed that the well-aligned TiO_2 nanotubular arrays well grew on the Ti substrate successfully in aqueous NH_4F electrolyte solution during such a low-voltage anodization process.

[Fig. 1]

3.2. Photocatalytic activity of TNT film

The photocatalytic activity of the TNT film was evaluated in terms of 2,3-DCP degradation in aqueous solution under UV illumination. A TiO_2 thin film with the same size was also prepared by the sol-gel method reported by Yu et al. (2001) and was heated at the same temperature of 500 ^{o}C for comparison, which had a nonporous structure and a film thickness of ~1.0 μm (not shown here). Two experiments were conducted under same experimental condition with an initial 2,3-DCP concentration of 20 mg L^{-1} and initial pH 5.3. The results are presented in Fig. 2. It can clearly be observed that after 300 min reaction while the TiO_2 film degraded 2,3-DCP by less than 40%, the TNT film achieved the much higher removal by 93% with a factor of about 2.6 times. Such higher reaction activity of TNT film might result from several factors of larger surface area, hollow interior walls, and a nanoscale-dimensional feature. It can be understood that when TiO_2 semiconductor is irradiated, electrons and holes are generated, but could recombine immediately. If the electrons and holes created do not recombine rapidly, they need to be either trapped in some metal-stable states or migrate to the semiconductor surface separately. The nanotube array architecture of the TNT film with a wall thickness of 28 nm ensures that the holes are never generated far from the semiconductor–electrolyte interface because the wall thickness is much less than the minority carrier diffusion length of $L_p \approx 100$ nm in TiO_2 (Hamnett, 1980), thus charge carrier separation takes place efficiently. In addition, the hollow feature of nanotubes enables the electrolyte species to permeate the entire internal and external surfaces. Paulose et al. (2006)

suggested that this could cause the holes to reach the electrolyte surface through diffusion, which takes place on a scale of picoseconds, and finally also reduce the bulk recombination. Besides these, the tube-to-tube contact points (~5 nm) presented in Fig. 1 may become another role responsible for the higher photoactivity for TNT film due to their quantum size effect and creation of a contact network between the nanotubes. This network let the charge carrier-transfer become easier and distance-longer. This hypothesis has been confirmed by Varghese and co-workers (2003). They stated that the nanoscale geometry of the nanotubes, in particular the tube-to-tube contact points, is believed to be responsible for the outstanding hydrogen gas sensitivity (Varghese et al., 2004). On the other hand, Lubberhuizen et al. (2000) also claimed that strong scattering inside the nanoporous network leads to a long effective path-length of photons and finally to very effective light absorption. Hence, complete light absorption is achieved in nanoporous films with a thickness considerably smaller than the light absorption depth in bulk material.

[Fig. 2]

3.3. Effect of DO

The effect of DO concentration on 2,3-DCP degradation with the initial concentration of 20 mg L^{-1} at initial pH 5.3 was investigated in two sets of experiments using the TiO_2 film and TNT film by purging N_2, air, or O_2 gas, respectively and the results are shown in Fig. 3. Figure 3 shows that after 300 min reaction under UV illumination, 2,3-DCP was degraded with the TiO_2 film by 49% at a high DO level of 33 mg L^{-1} (O_2), by 37% at a medium level of 8.1 mg L^{-1} (air), and by 29% at a low level of 0.3 mg L^{-1} (N_2), respectively. It is evident that for the TiO_2 film, increasing the DO concentration in the solution significantly increases the extent of 2,3-DCP degradation. Meanwhile, even at the very low DO concentration (N_2) the reaction rate was still significant. The similar result about the photocatalytic degradation of 4-chlorobenzoic acid using a TiO_2 thin film in a rotating disk photocatalytic reactor was also observed (Dionysiou et al., 2002). It has been reported that when molecular oxygen is used as an electron acceptor to trap and remove electrons from the surface of the titania particles for minimizing the build-up of free electrons, the reaction of adsorbed oxygen with photo-generated electrons at the surface of the titania catalyst is relatively slow and may be the rate-controlling step in photocatalytic oxidation reactions (Gerischer and Heller, 1991). Therefore, increasing the charge transfer rate from titania to

molecular oxygen will increase the efficiency of photocatalysis for organic substrate photo-oxidation. If the adsorbed oxygen is in excess of the photo-generated electrons at the surface, the rate of electron transfer to molecular oxygen will be maximized. However, they are affected by the types and characteristics of titania through the efficiency of electron–hole generation, recombination, and also charge transfer reaction rates (Almquist and Biswas, 2001).

For the TNT film, it can be seen from Fig. 3 that, at the very low DO concentration (N_2), the removal of 2,3-DCP was achieved by as high as 81% after 300 min reaction. The large decay of 2,3-DCP should be due to the unique nanotubular structure of TNT film, which owns a better separation of electron-hole and allows more efficient channeling of the charge carriers into the photochemical reactions, in spite of the absence of electron acceptor. Furthermore, the decomposition of 2,3-DCP increases to 93% in the presence of air and rises to 95% in the presence of oxygen, respectively. Only a slight enhancement of 2% from air to O_2 gas indicates that an air saturated water system can provide sufficient electron scavengers to accelerate the photocatalytic reaction using the TNT film under UV illumination.

[Fig. 3]

3.4. Effect of pH

Solution pH is one of the most important parameters that influence the photocatalytic reactions. To study the effect of pH on the photocatalytic degradation of 2,3-DCP, one set of experiments was carried out under same experimental conditions, but different initial pH in the range of 3.4-10.9. The experimental results are shown in Table 1. It is evident that at initial pH 3.4, the pseudo-first-order rate constant (k) of 2,3-DCP degradation was only 7×10^{-3} min^{-1} and the solution pH varied from 3.4 to 3.0 after 300 min UV irradiation. Instead, at initial pH 10.9 the k value reached 24×10^{-3} min^{-1} (3.4 times higher than that at pH 3.4) and the corresponding pH of the solution dropped from 10.9 to 7.1. The results in Table 1 demonstrated that 2,3-DCP was degraded faster at the higher pH and some acidic products were formed from the 2,3-DCP degradation.

[Table1]

216 In general, medium pH has a complex effect on the photodegradation rates of chlorophenols
217 depending on different molecular structures of chlorophenols as well as the semiconductors used
218 in the oxidation process. Several researches showed that the removal efficiency of chlorophenols
219 decreased with increasing pH values (Ku et al., 1996; Leyva et al., 1998; Quan et al., 2007). It is
220 suggested that TiO_2 surface carries a net positive charge (pH_{zpc} 6.25) at low pH value, while the
221 chlorophenols and intermediates are negatively charged naturally. Because of this, low pH value
222 can facilitate the adsorption of the organic compounds and promote better photocatalytic
223 degradation. In contrast, better removal efficiency of chlorophenols in alkaline condition has also
224 been reported (Stafford et al., 1994; Serpone et al., 1995; Doong et al., 2001), which is consistent
225 with our results. It is explained that the higher pH value can provide more hydroxide ions (OH^-) to
226 react with holes to form hydroxyl radicals, subsequently enhancing the degradation rate of
227 substituted phenols. The photocatalytic transformation of chlorophenols does not involve the •OH
228 oxidation exclusively and direct electron transfer and surface adsorption reactions also contribute
229 the disappearance of chlorophenols in TiO_2 (Stafford et al., 1994). Since the effect of pH can not
230 be generalized, Gogate and Pandit (2004) recommended that laboratory scale studies are required
231 for establishing the optimum pH conditions unless data are available in the literatures with exactly
232 similar operating conditions. In our case, the faster 2,3-DCP degradation occurring at the higher
233 pH may be attributed to two reasons: (1) more hydroxyl radicals are formed in alkaline solution
234 with more OH^- ions; and (2) it is easier for 2,3-DCP to absorb UV light energy at high pH, when
235 the functional group of phenol is dissociated to the phenate ion due to its $pK_a = 7.7$ (Tehan et al.,
236 2002) and the kinetic reaction constant has been found to be greater by several orders of
237 magnitude (Langlais et al., 1991). The much higher reactivity of the dissociated compounds at the
238 higher pH is believed to be via the attack of electrophilic species such as •OH radicals on the
239 phenate ion, which should be faster with a greater electron density on the aromatic ring. In contrast,
240 at low pH the undissociated species ($C_6H_3Cl_2OH$) is predominant. The hydrogen atom in polar O–
241 H bond and the electronegative chlorine atom on o-chlorophenol may form intramolecular
242 hydrogen bonding (O–H· · ·Cl) and develop a stable 5-membered ring. This hypothesis has been
243 supported by a number of literature precedents (Brune et al., 1999; Kolla et al., 2004). By taking
244 into account these, a possible coordination can be found in Scheme 1. In this way, there is an
245 increase of the o-chlorophenol resonance structure in the ground electronic state and at the same
246 time, an increase of the surroundings rigidity occurs due to formation of the chelate ring. Both

247 effects may resist the attack of •OH radicals on the protonated phenol ring at low pH condition,
248 evidently mirroring a corresponding decrease of the 2,3-DCP degradation.
249
250 [Scheme 1]
251
252 Table 1 also illustrates the pH dependency of the dechlorination of 2,3-DCP and DOC reduction
253 using the TNT film. Similar to its degradation, the photocatalytic dechlorination of 2,3-DCP was
254 observed to be faster at alkaline pH than that at acidic pH (pH 10.9 > 7.8 > 5.3 > 3.4). However,
255 DOC reduction demonstrated an opposite result on the pH dependency, in which the
256 photocatalytic reaction at initial pH 10.9 after 300 min UV irradiation lead to a significant release
257 of chloride by 99% , whereas the loss of DOC was only 20%. In the case of acidic pH (pH 3.4 and
258 5.3), the dechlorination of 2,3-DCP was only 52% and 57% after 300 min, whereas the reduction
259 of DOC reached 47% and 40%, respectively. These results indicate that acidic condition is more
260 favorable for the 2,3-DCP mineralization (further degradation) rather than its decomposition
261 (initial degradation). This may be mainly attributed to the formation of organic intermediates in
262 the photocatalytic reaction. Information on the intermediate concentrations at different pH and the
263 pathway of 2,3-DCP degradation has been studied through the ^{1}H-NMR analysis as shown in
264 Table 2.
265 Table 2 shows the ^{1}H-NMR spectral data of residual aromatic compounds and their corresponding
266 concentrations at 12 h irradiation time for the photodegradation of 2,3-DCP with an initial
267 concentration of 300 mg L^{-1} with different initial pH. It was clearly observed that the distribution of
268 intermediates of 2,3-DCP was pH-dependent. Compound like 2-chlororesorcinol is the major
269 intermediate from the decomposition of 2,3-DCP under three pH conditions (pH 3.4, 5.3, and 10.9).
270 For example, the concentration of 2-chlororesorcinol at pH 10.9 reached 90 mg L^{-1}, which was
271 critically higher than those at pH 3.4 (12.6 mg L^{-1}) and 5.3 (18.9 mg L^{-1}). Furthermore, at pH 10.9
272 the total concentration of residual compounds in the irradiated solution (including the residual 2,3-
273 DCP and compounds 1-7) is obviously higher than those at pH 3.4 and 5.3. This accumulated
274 amount of 2-chlororesorcinol indicated its degradation more slowly under an alkaline condition
275 rather than that under an acidic condition, resulting in a lower DOC reduction under the alkaline
276 condition. Furthermore, the different concentration distribution of intermediates detected at different
277 pH values indicates that the solution media is susceptible to OH attack on the aromatic moiety.

Based on the organic intermediates identified by the ^{1}H-NMR analysis, a possible pathway of 2,3-DCP degradation in this reaction system can be proposed as shown in Fig. 4. The reactions may mainly involve the addition of hydroxyl radicals to the organic substrate by three approaches of (a) hydroxylation of the aromatic ring, (b) substitution of chlorine by OH, and (c) oxidation of hydroxylated hydroquinone to the corresponding quinine (Antonaraki et al., 2002). The routes (a) and (b) in Fig. 4 was based on the dechlorination process, where the •OH substitution removes the chlorine in the ring, leading to form the hydroxyl derivatives (compounds **1**, **2**, and **5**). Due to the stereochemical inhibition of *ortho*-chlorosubstituents, compound **1** is the major intermediate from the 2,3-DCP decomposition under three pH conditions.

In general, the OH groups in the chlorophenol ring are *ortho* and *para* directing with activation, whereas Cl substituents are *ortho* and *para* directing with deactivation. When the OH radical, an electrophilic reagent, is attacking 2,3-DCP, it is expected to attack the electron rich positions and cause to generate major *para*- or *ortho*-substituted intermediates (i.e. 3-chlorocatechol, 3,4-dichlorocatechol, and 2,3-dichloroquinol). This seems to be the case of this study. Besides the *para*- or *ortho*-substituted intermediates in present paper, however, a new intermediate, 2-chlororesorcinol, with the highest concentration was observed as *meta*-substituted intermediate under three pH conditions, which is different from the previous report (D'Oliveira et al., 1993). This indicates that this ring position is attacked by •OH radical preferentially. This can be attributed to the strong stereochemical inhibition of *ortho*-chlorosubstituents to •OH radical attack, due to the close proximity of OH and Cl groups on the aromatic ring (Tang and Huang, 1995) and/or to the formation of intramolecular hydrogen bonding between the OH and Cl groups in the aromatic ring (mentioned above). As a result, compound corresponding to a primary OH substitution at the *meta*-position was detected.

In the routes (c) and (d), the detected intermediates are all rationalized as being formed by hydrogen abstraction, followed by *para*- and *ortho*-hydroxylation of the ring, respectively. Hydroxyl radicals attack preferentially the aromatic moiety due to their electrophilic character to form the hydroxylated compounds **3** and **4**. The two products are then followed to dechlorinate through the •OH attack (compound **6**) and finally oxidized to corresponding quinine (compound **7**).

[Table 2]

[Fig. 4]

3.5. Effect of anions

The existence of inorganic anions such as chloride, sulfate, carbonate, nitrate, and phosphate is considerably common in wastewaters and also in natural water. The importance of anions effect on the photodegradation of pollutants has been remarkably recognized due to the occurrence of the competitive adsorption, resulting in the inhibitive effect on the photoreaction of organic pollutants. In this study, the initial pH 5.3 was employed and the effect of Cl^- on the photocatalytic degradation of 2,3-DCP in the TNT/UV system was first studied by adding NaCl into the reaction solution at different concentrations of 0.005, 0.05 and 0.1 M, The results are shown in Fig. 5a. It can be seen that while the removal of 2,3-DCP without any anion was achieved by 93% after 300 min UV irradiation, it was achieved by 77% only at $[Cl^-] = 0.005$ M, and further down to 64% at $[Cl^-] = 0.1$ M. This indicates that the rate of 2,3-DCP degradation decreased with an increased Cl^- concentration significantly. The observed inhibition effect is often explained by competitive adsorption (Chen et al., 1997). To understand the adsorption behavior of the TNT catalyst in aqueous solution, the TiO_2 nanotubes were peeled off from the TNT films and a powdery suspension was prepared to measure its point of zero charge (pzc) in the pH range of 3.3–10.7 as shown in Fig. 6, where P25 powder with the same concentration was also used as the reference. It can be seen that the pzcs of P25 and TNT samples were at pH 6.21 and 5.23, respectively. The results demonstrated that the isoelectric point of TNT catalyst was very close to the reported value of pH 5.3 (Wang et al., 2006) and lower than that of P25 powder. In fact, the photocatalytic process mainly occurs on the photocatalyst surface, but not in the bulk solution. It is suggested that the isoelectric point would greatly influence the adsorption of organic substrates and its intermediates on the surface of photocatalyst during photoreaction (Hu et al., 2001). Therefore, the TiO_2 nanotube surface is positively charged at pH < 5.2, and Cl^- can be easily adsorbed onto the positively charged surface of the catalyst by electrostatic attraction, leading to the competitive adsorption.

[Fig. 5]

[Fig. 6]

The other probability is that chloride ions can act as scavengers of positive holes (h^+) and/or hydroxyl radical (•OH) through the following reactions:

$$Cl^- + h^+ \rightarrow Cl\bullet \quad (1)$$

$$\bullet OH + Cl^- \rightarrow Cl\bullet + OH^- \quad (2)$$

Meanwhile, the dichloride radical anion $Cl_2\bullet^-$ from the further reaction of Cl• with Cl^- (Eq. 3) is reactive with organic substances and the recombination of two chloride radicals $Cl\bullet/Cl_2\bullet^-$ (Eqs. 4 and 5) (Rincón and Pulgarin, 2004) are the source of molecular chlorine, thus ending the radicals transfer.

$$Cl\bullet + Cl^- \rightarrow Cl_2\bullet^- \quad (3)$$

$$Cl_2\bullet^- + Cl_2\bullet^- \rightarrow Cl_2 + 2Cl^- \quad (4)$$

$$Cl\bullet + Cl\bullet \rightarrow Cl_2 \quad (5)$$

Since Cl• is less reactive than •OH, the excess Cl^- may have the inhibition effect on the photodegradation of 2,3-DCP in aqueous solution.

Figure 5b shows the effects of different anions (i.e. Cl^-, NO_3^-, $H_2PO_4^-$, and SO_4^{2-}) at the same concentration of 0.05 M. Compared to the control test in the aqueous 2,3-DCP solutions without anion, the existence of all anions reduced the 2,3-DCP degradation to a certain degree. Among them, the strongest inhibition of 2,3-DCP degradation resulted from SO_4^{2-} due to its ionic properties. At pH < 5.3, like Cl^-, SO_4^{2-} can inhibit the photodegradation of the chlorophenol through two ways of: (1) competitive adsorption with the 2,3-DCP on the TNT film surface due to the higher ionic strength and (2) trapping positive holes and/or hydroxyl radical, where SO_4^{2-} can be led to the generation of less reactive radical $SO_4\bullet^-$. Actually, the divalence charge for SO_4^{2-} can lead to the stronger binding of the SO_4^{2-} with the catalyst, as compared with the single valence ions such as NO_3^-, Cl^-, and $H_2PO_4^-$, thus resulting in the stronger competitive adsorption. For the addition of $H_2PO_4^-$, the behavior of $H_2PO_4^-$ ions is similar to SO_4^{2-} ions, in that the $H_2PO_4^-$ reacted with h^+ and •OH to form $H_2PO4\bullet^-$, less reactive than that of h^+ and •OH. Formation of inorganic radical anions under these circumstances was also reported in some literatures (Abdullah et al., 1990; Bekbölet et al., 1998; Hu et al., 2003). The addition of NO_3^- to the solution in this

study showed a minor effect on the photocatalytic degradation of 2,3-DCP only. Abdullah et al. (1990) also reported that the presence of $NaNO_3$ had negligible effect on the photodegradation of ethanol and 2-propanol under UV light irradiation. On the basis of above discussion, the observed inhibition effect may be therefore explained by combination of the competitive adsorption and the formation of less reactive radicals during the photocatalytic reaction.

4. Conclusions

The highly-ordered TiO_2 nanotube arrays were successfully formed on Ti foil by an anodic oxidation method. The experimental results showed that the anodic TNT film had the higher photocatalytic activity than the conventional TiO_2 thin film prepared by a sol-gel method with a factor of about 2.6 times. DO acts as an effective electron acceptor to extend the hole's lifetime and to form the oxidizing species of •OH radicals, affecting the photoactivity of the TNT film. Effect of solution pH demonstrated that an alkaline condition is favorable to 2,3-DCP degradation and dechlorination, but an acidic condition is more beneficial to further mineralization. The presence of NO_3^- had a weak inhibition effect on the degradation of 2,3-DCP, while SO_4^{2-} had the strongest inhibition.

Acknowledgements

The authors wish to acknowledge the support of the Research Committee of The Hong Kong Polytechnic University in providing a PhD scholarship for H. C. Liang.

References

Abdullah, M., Low, K.C., Mattheus, R.W., 1990. Effects of common inorganic anions on rates of photocatalytic oxidation of organic carbon over illuminated titanium dioxide. J. Phys. Chem. 94, 6820-6825.

Almquist, C.B., Biswas, P., 2001. A mechanistic approach to modeling the effect of dissolved oxygen in photo-oxidation reactions on titanium dioxide in aqueous systems. Chem. Eng. Sci. 56, 3421-3430.

399 Antonaraki, S., Androulaki, E., Dimotikali, D., Hiskia, A., Papaconstantinou, E., 2002. Photolytic
400 degradation of all chlorophenols with polyoxometallates and H_2O_2. J. Photochem. Photobiol.
401 A 148, 191-197.
402 Arabatzis, I.M., Antonaraki, S., Stergiopoulos, T., Hiskia, A., Papaconstantinou, E., Bernard, M.C.,
403 Falaras, P., 2002. Preparation, characterization and photocatalytic activity of nanocrystalline
404 thin film TiO_2 catalysts towards 3,5-dichlorophenol degradation. J. Photochem. Photobiol. A
405 149, 237-245.
406 Bekbölet, M., Boyacioglu, Z., Özkaraova, B., 1998. The influence of solution matrix on the
407 photocatalytic removal of color from natural waters. Water Sci. Technol. 38(6), 155-162.
408 Bellar, J.A., Lichtenberg, J.J., Kroner, R.C., 1974. The occurrence of organohalides in chlorinated
409 drinking waters. J. Am. Water Works Ass. 66(22), 703-706.
410 Brune, B.J., Koehler, J.A., Smith, P.J., Payne, G.F., 1999. Correlation between adsorption and
411 small molecule hydrogen bonding. Langmuir 15, 3987-3992.
412 Chen, H.Y., Zahraa, O., Bouchy, M., 1997. Inhibition of the adsorption and photocatalytic
413 degradation of an organic contaminant in an aqueous suspension of TiO_2 by inorganic ions. J.
414 Photochem. Photobiol. A 108, 37-44.
415 Dionysiou, D.D., Burbano, A.A., Suidan, M.T., Baudin, I., Laîné, J.M., 2002. Effect of oxygen in
416 a thin-film rotating disk photocatalytic reactor. Environ. Sci. Technol. 36, 3834-3843.
417 D'Oliveira, J.C., Minerob, C., Pelizzettib, E., Pichat, P., 1993. Photodegradation of
418 dichlorophenols and trichlorophenols in TiO_2 aqueous suspensions: kinetic effects of the
419 positions of the Cl atoms and identification of the intermediates. J. Photochem. Photobiol. A
420 72, 261-267.
421 Doong, R.A., Chen, C.H., Maithreepala, R.A., Chang, S.M., 2001. The influence of pH and
422 cadmium sulfide on the photocatalytic degradation of 2-chlorophenol in titanium dioxide
423 suspensions. Water Res. 35, 2873-2880.
424 Eder, D., Kinloch, I.A., Windle, A.H., 2006. Pure rutile nanotubes. Chem. Commun. 13, 1448-
425 1450.
426 Gerischer, H., Heller, A., 1991. The role of oxygen in photooxidation of organic molecules on
427 semiconductor particles. J. Phys. Chem. 95, 5261-5267.
428 Gogate, P.R., Pandit, A.B., 2004. A review of imperative technologies for wastewater treatment I:
429 Oxidation technologies at ambient conditions. Adv. Environ. Res. 8, 501-551.

430 Gracia, F., Holgado, J.P., González-Elipe, A.R., 2004. Photoefficiency and optical, microstructural,
431 and structural properties of TiO_2 thin films used as photoanodes. Langmuir 20, 1688-1697.
432 Hagfeldt, A., Grätzel, M., 1995. Light-induced redox reactions in nanocrystalline systems, Chem.
433 Rev. 95 (1995) 49–54.
434 Hahn, R., Stergiopoulus, T., Macak, J.M., Tsoukleris, D., Kontos, A.G., Albu, S.P., Kim, D.,
435 Ghicov, A., Kunze, J., Falaras, P., Schmuki, P., 2007. Efficient solar energy conversion using
436 TiO_2 nanotubes produced by rapid breakdown anodization – A comparison. Phys. Stat. Sol.
437 (RRL) 1, 135-137.
438 Hamnett, A., 1980. Porous-electrodes for water oxidation. Faraday Discuss. Chem. Soc. 70, 127-
439 134.
440 Hu, C., Wang, Y.Z., Tang, H.X., 2001. Influence of adsorption on the photodegradation of various
441 dyes using surface bond-conjugated TiO_2/SiO_2 photocatalyst. Appl. Catal. B-Environ. 35, 95-
442 105.
443 Hu, C., Yu, J.C., Hao, Z., Wong, P.K., 2003. Effects of acidity and inorganic ions on the
444 photocatalytic degradation of different azo dyes. Appl. Catal. B-Environ. 46, 35-47.
445 Kinzell, L.H., McKenzie, R.M., Olson, B.A., Kirsch, D.G., Shull, L.R., 1979. Priority pollutants, I:
446 A perspective view. Environ. Sci. Technol. 13, 416-423.
447 Kolla, A., Parasukb, V., Parasukc, W., Karpfend, A., Wolschann, P., 2004. Theoretical study on
448 the intramolecular hydrogen bond in chloro-substituted N,N-dimethylaminomethylphenols. I.
449 Structural effects. J. Mol. Struct. 690, 165-174.
450 Ku, Y., Leu, R.M., Lee, K.C., 1996. Decomposition of 2-chlorophenol in aqueous solution by UV
451 irradiation with the presence of titanium dioxide. Water Res. 30, 2569-2578.
452 Lagemaat, J., Plakman, M., Vanmaekelbergh, D., Kelly, J.J., 1996. Enhancement of the light-to-
453 current conversion efficiency in an n-SiC/solution diode by porous etching, Appl. Phys. Lett.
454 69, 2246-2248.
455 Langlais, B., Reckhow, D.A., Brink, R.B. (Eds.), 1991. Ozone in water treatment—Application
456 and engineering. Lewis Publishers, Chelsea, USA, pp. 43-45.
457 Leyva, E., Moctezuma, E., Ruíz, M.G., Martínez, L., 1998. Photodegradation of phenol and 4-
458 chlorophenol by $BaO–Li_2O–TiO_2$ catalysts. Catal. Today 40, 367-376.
459 Lubberhuizen, W.H., Vanmaekelbergh, D., Van Faassen, E., 2000. Recombination of
460 photogenerated charge carriers in nanoporous gallium phosphide, J. Porous Mater. 7, 147-152.

Mor, G.K., Shankar, K., Paulose, M., Varghese, O.K., Grimes, C.A., 2005. Enhanced photocleavage of water using titania nanotube arrays. Nano Lett. 5, 191-195.

Mor, G.K., Varghese, O.K., Paulose, M., Ong, K.G., Grimes, C.A., 2006. Fabrication of hydrogen sensors with transparent titanium oxide nanotube-array thin films as sensing elements. Thin Solid Films 496, 42-48.

Paulose, M., Mor, G.K., Varghese, O.K., Shankar, K., Grimes, C.A., 2006. Visible light photoelectrochemical and water-photoelectrolysis properties of titania nanotube arrays. J. Photochem. Photobiol. A 178, 8-15.

Quan, X., Ruan, X.L., Zhao, H.M., Chen, S., Zhao, Y.Z., 2007. Photoelectrocatalytic degradation of pentachlorophenol in aqueous solution using a TiO_2 nanotube film electrode. Environ. Pollut. 147, 409-414.

Quan, X., Yang, S.G., Ruan, X.L., Zhao, D.M., 2005. Preparation of titania nanotubes and their environmental applications as electrode. Environ. Sci. Technol. 39, 3770-3775.

Rincón, A.G., Pulgarin, C., 2004. Effect of pH, inorganic ions, organic matter and H_2O_2 on *E. coli* K12 photocatalytic inactivation by TiO_2 implications in solar water disinfection. Appl. Catal. B-Environ. 51, 283-302.

Serpone, N., Maruthamuthu, P., Pichat, P., Pelizzetti, E., Hidaka, H., 1995. Exploiting the interparticle electron transfer process in the photocatalyzed oxidation of phenol, 2-chlorophenol and pentachlorophenol: chemical evidence for electron and hole transfer between coupled semiconductors. J. Photochem. Photobiol. A 85, 247-255.

Stafford, U., Gray, K.A., Kamat, P.V., 1994. Radiolytic and TiO_2-assisted photocatalytic degradation of 4-chlorophenol. A comparative study. J. Phys. Chem. 98, 6343-6351.

Sukamto, J.P.H., Smyrl, W.H., Mcmillan, C.S., Kozlowski, M.R., 1992. Photoelectrochemical measurements of thin oxide-films—multiple internal-reflection effects. J. Electrochem. Soc. 139, 1033-1043.

Tang, W.Z., Huang, C.P., 1995. The effect of chlorine position of chlorinated phenols on their dechlorination kinetics by Fenton's reagent. Waste Manage. 15, 615-622.

Tehan, B.G., Lloyd, E.J., Wong, M.G., Pitt, W.R., Montana, J.G., Manallack, D.T., Gancia, E., 2002. Estimation of pK_a using semiempirical molecular orbital methods. Part 1: Application to phenols and carboxylic acids. Quant. Struct-Act. Rel. 21, 457-472.

Uchikoshi, T., Suzuki, T.S., Tang, F., Okuyama, H., Sakka, Y., 2004. Crystalline-oriented TiO_2 fabricated by the electrophoretic deposition in a strong magnetic field. Ceramic Inter. 30, 1975-1978.

Varghese, O.K., Gong, D., Paulose, M., Ong, K.G., Dickey, E.C., Grimes, C.A., 2003. Extreme changes in the electrical resistance of titania nanotubes with hydrogen exposure. Adv. Mater. 15, 624-627.

Varghese, O.K., Mor, G.K., Grimes, C.A., Paulose, M., Mukherjeeb, N., 2004. A titania nanotube-array room-temperature sensor for selective detection of hydrogen at low concnetrations. J. Nanosci. Nanotechnol. 4, 733-737.

Wang, N., Lin, H., Li, J.B., Yang, X.Z., Chi, B., 2006. Electrophoretic deposition and optical property of titania nanotubes films. Thin Solid Films 496, 649-652.

Xie, Y.B., 2006. Photoelectrochemical application of nanotubular titania photoanode. Electrochim. Acta 51, 3399-3406.

Ye, F.X., Shen, D.S., 2004. Acclimation of anaerobic sludge degrading chlorophenols and the biodegradation kinetics during acclimation period. Chemosphere 54, 1573-1580.

Yu, J.G., Zhao, X.J., Zhao, Q.N., 2001. Photocatalytic activity of nanometer TiO_2 thin films prepared by the sol–gel method. Mater. Chem. Phys. 69, 25-29.

Zheng, S.K., Yang, Z.F., Job, D.H., Yun Hee Park, Y.H., 2004. Removal of chlorophenols from groundwater by chitosan sorption. Water Res. 38, 2315-2322.

Zhuang, H.F., Lin, C.J., Lai, Y.K., Sun, L., Li, J., 2007. Some critical structure factors of titanium oxide nanotube array in its photocatalytic activity. Environ. Sci. Technol. 41, 4735-4740.

List of figure captions

Fig. 1. (a) FESEM images of TNT film; (b) XRD patterns of Ti foil and TNT film calcined at 500 ^{o}C for 1 h.

Fig. 2. 2,3-DCP degradation with TiO_2 film and TNT film under UV illumination (Initial pH 5.3 and $[C_o]$ = 20 mg L^{-1}).

Fig. 3. Effect of DO concentration on 2,3-DCP degradation with TiO_2 film and TNT film by blowing different gases (N_2, air or O_2), respectively (Initial pH 5.3 and $[C_o]$ = 20 mg L^{-1}).

Fig. 4. Pathway of the 2,3-DCP degradation in the TNT/UV system.

Fig. 5. (a) Influence of Cl^- concentrations on the photocatalytic deactivation of TNT/UV system (Initial pH 5.3 and $[C_o]$ = 20 mg L^{-1}); (b) Photocatalytic deactivation in the presence of different anions at 0.05 M (Initial pH 5.3 and $[C_o]$ = 20 mg L^{-1}): (●) no anion; (■) NO_3^-; (▲) $H_2PO_4^-$; (▼) Cl^-; (♦) SO_4^{2-}.

Fig. 6. Zeta potential analysis of P25 and TNT samples as a function of pH.

Scheme 1. Formation of intramolecular hydrogen bonding in 2,3-DCP molecular structure.

537 Fig. 1.

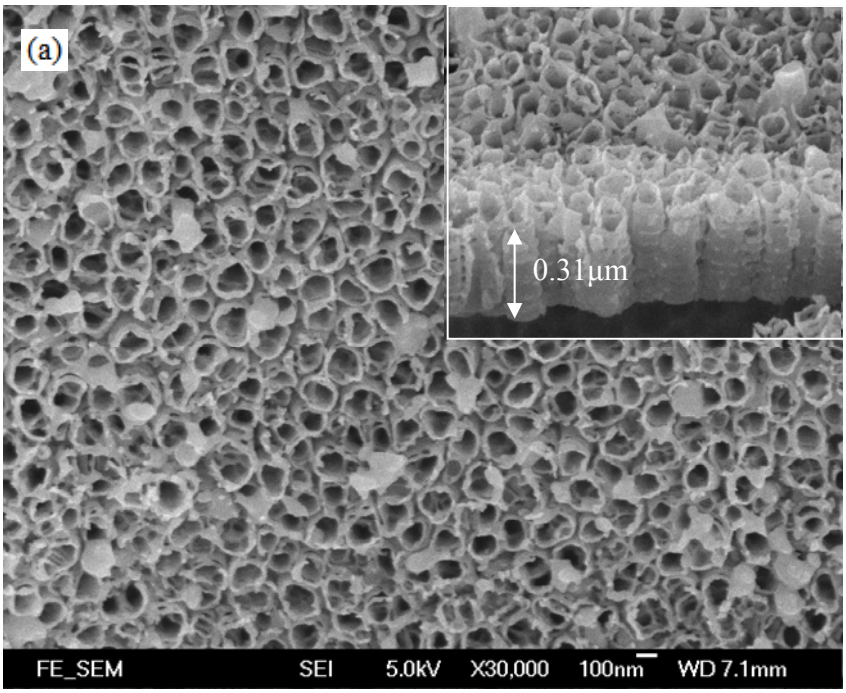

538

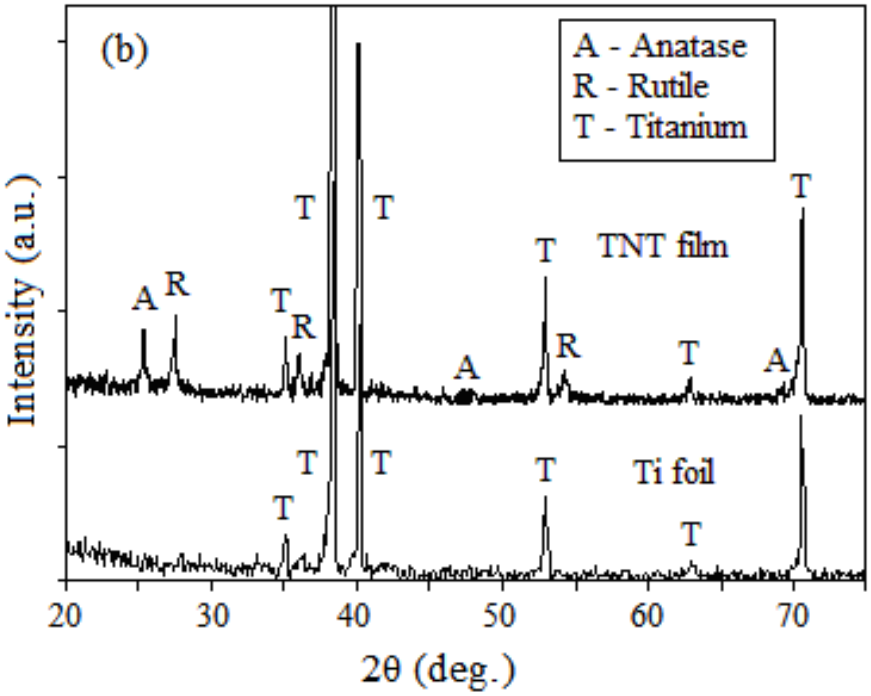

539

540

541

Fig. 2

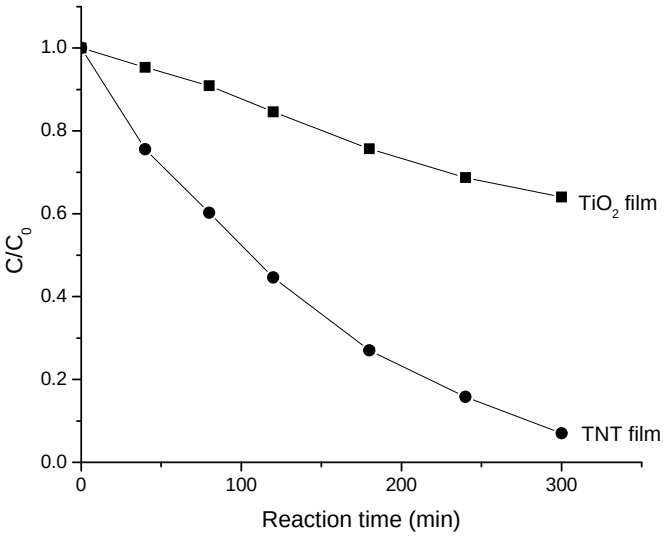
1.0
0.8
0.6
0.4
0.2
0.0
C/C0
0
100
200
300
Reaction time (min)
TiO2 film
TNT film

Fig. 3

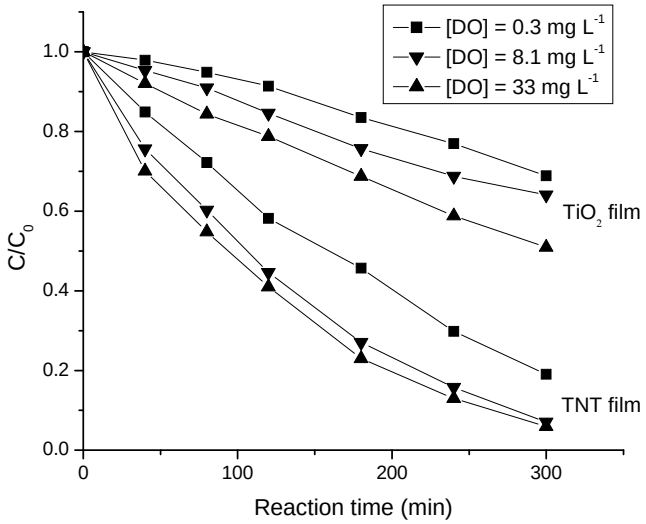
[DO] = 0.3 mg L-1
[DO] = 8.1 mg L-1
[DO] = 33 mg L-1
TiO2 film
TNT film
C/C0
Reaction time (min)
0.0
0.2
0.4
0.6
0.8
1.0
0
100
200
300

Fig. 4

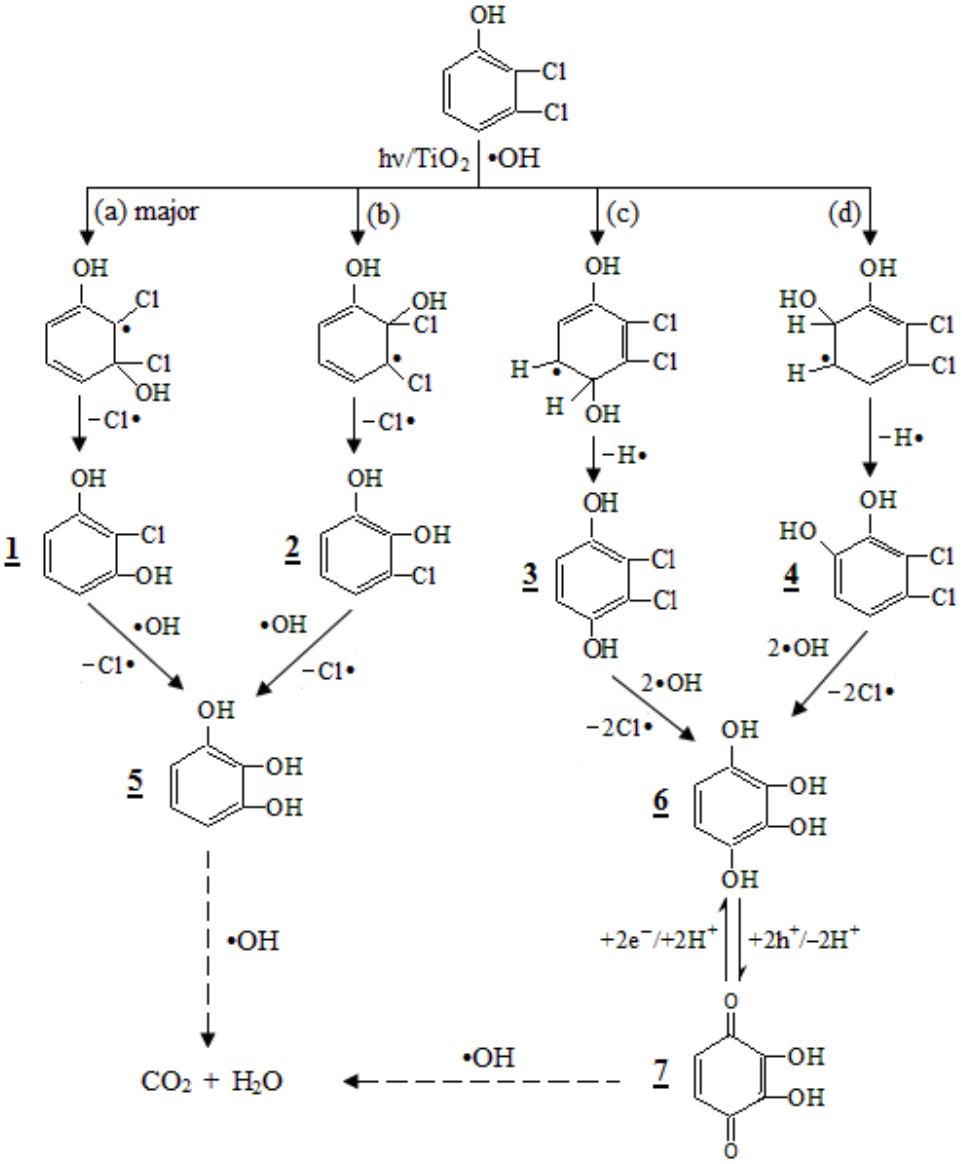
OH
Cl
Cl
hν/TiO2 •OH
(a) major
(b)
(c)
(d)
−Cl•
−Cl•
−H•
−H•
1
2
3
4
•OH
−Cl•
•OH
−Cl•
2•OH
−2Cl•
2•OH
−2Cl•
5
6
•OH
+2e−/+2H+
+2h+/−2H+
7
•OH
CO2 + H2O

584

585

586 Fig. 5

587

588

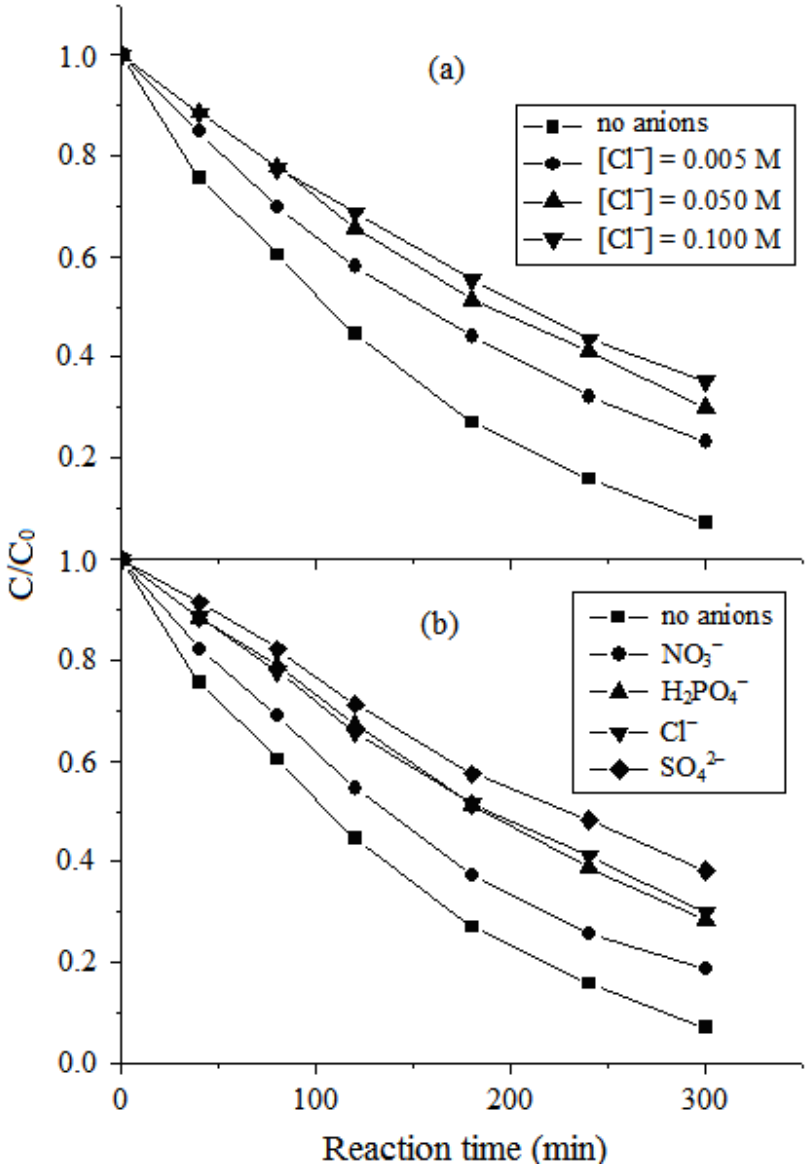

589

590

591

592

593

Fig. 6

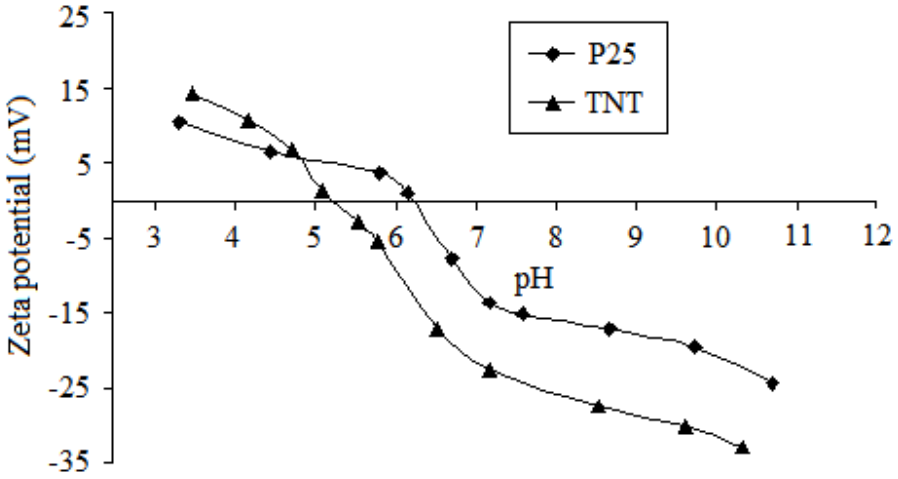

601

602 Scheme 1.

603

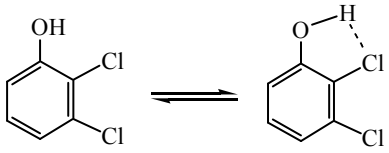

604

605

606

607

608

609

610

611

612

613

614

615

616
617
618 Table 1
619 Effect of solution pH on the 2,3-DCP degradation, dechlorination, and DOC removal after 300
620 min reaction

Test No.	pH		2,3-DCP degradation[a]		Dechlorination[b]	DOC reduction
	Initial	Final	k (min^{-1})	(%)	(%,Cl^-/Cl_{total})	(%)
1	3.4	3.0	0.007	90	52	47
2	5.3	3.4	0.008	93	57	40
3	7.8	3.8	0.011	96	74	37
4	10.9	7.1	0.024	100	99	20

621
622 [a] Photocatalytic degradation of 2,3-DCP was thought to be a pseudo-first-order reaction; k is the
623 kinetic constant.
624 [b] Dechlorination was calculated on the basis of the total chlorine (Cl^-/Cl_{total}) in 2,3-DCP of 20 mg
625 L^{-1}.
626
627
628
629
630
631
632
633
634
635
636
637
638
639
640

641 Table 2

642 Identification of intermediates from 2,3-DCP degradation by ^{1}H-NMR analysis

Compound[a] No.	Proton	Chemical shifts (ppm)	Description[b]	Concentrations (mg L^{-1}) pH 3.4	pH 5.3	pH 10.9
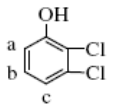 (2,3-dichlorophenol)	a b c	6.97 7.18 7.13	1H, d, J_{ab} = 9.85 1H, m, 1H, d, J_{cb} = 8.34	47.2	47.2	26.0
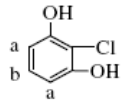 (2-chlororesorcinol)	a b	6.62 7.09	2H, d, J_{ab} = 9.1 1H, t, J_{ba} = 9.1	12.6	18.9	90.1
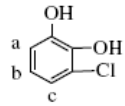 (3-chlorocatechol)	a b c	6.52 6.82 6.86	1H, d, J_{ab} = 8.9 1H, m, 1H, d, J_{bc} = 8.9	8.4	12.6	2.1
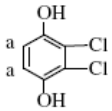 (2,3-dichloroquinol)	a	6.75	1H, s	2.3	2.3	2.3
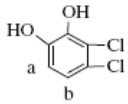 (5,6-dichlorocatechol)	a b	6.46 6.95	1H, d, J_{ab} = 8.7 1H, d, J_{ba} = 8.8	trace	trace	6.9
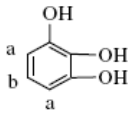 (Pyrogallol)	a b	6.40 6.61	2H, d, J_{ab} = 8.3 1H, t, J_{ba} = 8.1	2.7	1.8	2.7
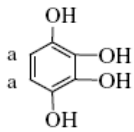 (1,2,3,4-benzenetetrol)	a	6.08	2H, s	4.2	2.1	10.5
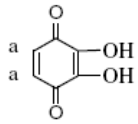 (2,3-dihydroxy-p-benzoquinone)	a	6.89	2H, s	1.7	1.7	1.6

643

644 [a] Different protons linked on benzene ring are marked as a, b, and c, respectively.

645 [b] Singlet, doublet, triplet, and multilet are abbrivated as s, d, t, and m, respectively; coupling

646 constants (*J*) are given hertz.